Computational Energy Science

Vol. 2, No. 4, p. 117-131, 2025

Original article

Density functional theory studies of nanomaterials for hydrogen storage

Remya Geetha Sadasivan Nair[1], Arun Kumar Narayanan Nair[1]*, Shuyu Sun[2], Bicheng Yan[1]*

[1]*Physical Science and Engineering Division (PSE), King Abdullah University of Science and Technology (KAUST), Thuwal, 23955-6900, Saudi Arabia.*

[2]*School of Mathematical Sciences, Tongji University, Shanghai 200092, P. R. China*

Keywords:
Hydrogen storage
adsorption
density functional theory

Cited as:
Nair, R. G. S., Nair, A. K. N., Sun, S., Yan, B. Density functional theory studies of nanomaterials for hydrogen storage. Computational Energy Science, 2025, 2(4): 117-131.
https://doi.org/10.46690/compes.2025.04.01

Abstract:
Density functional theory studies were carried out to understand the interactions between H_2 and nanomaterials such as pristine and Li/Ca/Pd-decorated graphene, h-BN nanosheet, h-AlN nanosheet, carbon nanotube (CNT), BNNT, AlNNT, C_{60} fullerene, $B_{12}N_{12}$ nanocage, $Al_{12}N_{12}$ nanocage, C_{18} nanoring, etc. Our results suggest that, in general, H_2 was weakly adsorbed on these nanomaterials. However, H_2 was strongly adsorbed on Pd-decorated nanomaterials. Importantly, the adsorption of H_2 on Li/Ca-decorated nanomaterials was often but not always enhanced. The lowest adsorption energy was found for the Li-decorated (8,0) BNNT (-0.01 kcal/mol) and the highest for the Pd-decorated $Al_{12}N_{12}$ nanocage (-21.95 kcal/mol). The QTAIM results showed a partial covalent character for the interactions of H_2 with Pd-decorated nanomaterials and $Al_{12}N_{12}$ nanocage, and a noncovalent character for the interactions of H_2 with other nanomaterials. In addition, an overview of the previous quantum chemical studies on the interactions between H_2 and such nanomaterials is presented. The Kubas-type (or orbital) interaction between H_2 and transition metal can lead to a significant adsorption energy. Transition metal atoms might cluster on the surface of the nanomaterial, which can reduce the weight percentage of H_2 storage. The interaction between H_2 and such metal-decorated nanomaterials might be enhanced by replacing the C/B/Al/N atoms with heteroatoms and by introducing vacancy defects.

1. Introduction

There is an emergency to develop alternative fuels because of the declining fossil fuel supply and the environmental harm caused by CO_2 emission (Langmi et al., 2005; Germain et al., 2009; Shevlin and Guo, 2009; Suh et al., 2012; Spyrou et al., 2013; Chung et al., 2015; Sawant et al., 2022; Shiraz and Tavakoli, 2017; Singla and Jaggi, 2021; Cruz-Martínez et al., 2024; Wang et al., 2025; Yao et al., 2025). Hydrogen is one of the most promising candidates to replace the current carbon-based fuels. Hydrogen fuel cells hold vast prospects in transportation and power generation applications. Hydrogen can be converted into energy in a fuel cell with the production of water as the only byproduct. Storage materials with high hydrogen storage capacities, reversible hydrogen storage, and low cost are preferred for fuel cell vehicles. The 2025 US Department of Energy (DOE) target is a hydrogen storage system with a gravimetric capacity of 0.055 kg H_2/kg system and a volumetric capacity of 0.040 kg H_2/L system (DOE, 2025). Several adsorbents such as metal-organic frameworks, nanoporous polymers, zeolites, graphene, and carbon nanotube (CNT) have emerged as promising candidates for hydrogen storage (Langmi et al., 2005; Germain et al., 2009; Shevlin and Guo, 2009; Suh et al., 2012; Spyrou et al., 2013; Chung et al., 2015; Shiraz and Tavakoli, 2017; Singla and Jaggi, 2021; Sawant et al., 2022; Cruz-Martínez et al., 2024; Wang et al., 2025; Yao et al., 2025).

Recently, the studies of the adsorption behavior of H_2 on different dimensional nanomaterials such as pristine and metal-decorated graphene, hexagonal-BN (h-BN) nanosheet,

Yandy Scientific Press

*Corresponding author.
E-mail address: remya.nair@kaust.edu. (R. G. S. Nair); arun.narayanannair@kaust.edu.sa (A. K. N. Nair); suns@tongji.edu.cn (S. Sun); bicheng.yan@kaust.edu.sa (B. Yan).

Received October 5, 2025; revised November 3, 2025; accepted December 5, 2025; available online December 10, 2025.

h-AlN nanosheet, CNT, BNNT, AlNNT, C_{60} fullerene, $B_{12}N_{12}$ nanocage, $Al_{12}N_{12}$ nanocage, cyclo[n]carbon (Cn nanoring), etc. have received significant attention. For instance, the experimentally determined adsorption energy of H_2 on graphite was about -1.0 kcal/mol (Mattera et al., 1980; Vidali et al., 1991). The experimentally determined adsorption energy of H_2 on some single-walled CNT bundles (-1.20 to -1.43 kcal/mol) was similar to that on graphite (Brown et al., 2000; Schimmel et al., 2003). Experimental studies have shown that BNNTs can be explored as a possible hydrogen storage medium (Ma et al., 2002; Tang et al., 2002). Furthermore, using density functional theory (DFT), Rubeš et al. (2010) reported that the adsorption distance and the adsorption energy for the H_2/graphene system were 3.06 Å and -1.30 kcal/mol, respectively (Rubeš and Bludský, 2009). Similar results were attained by other theoretical studies (Yeamin et al., 2014; de Lara-Castells and Mitrushchenkov, 2015; Bartolomei et al., 2017; Petrushenko and Petrushenko, 2019). The interaction of H_2 with BNNT, which is normally very weak, can be significantly enhanced upon functionalization by metal atoms such as Ti and Pd (Durgun et al., 2007; Zhang et al., 2011). The metal atoms can cluster on the surface of the nanomaterials, thus undermining their ability to store hydrogen. This problem can be eased by introducing heteroatoms and/or vacancy defects (Wang et al., 2025). We recently showed that the adsorption distance and the adsorption energy for the $H_2/B_{12}N_{12}$ system were 2.67 Å and -0.83 kcal/mol, respectively (Nair et al., 2024). However, the adsorption properties of H_2 on, for example, Pd-decorated h-AlN nanosheet and $B_{12}N_{12}$ nanocage are yet to be investigated.

In the present work, we investigate the adsorption behavior of H_2 on nanomaterials such as pristine and lithium/calcium/palladium-decorated graphene, h-BN nanosheet, h-AlN nanosheet, carbon nanotube (CNT), BNNT, AlNNT, C_{60} fullerene, $B_{12}N_{12}$ nanocage, $Al_{12}N_{12}$ nanocage, C_{18} nanoring, etc. using DFT. Our results indicate that overall H_2 is weakly adsorbed on these nanomaterials. However, H_2 is strongly adsorbed on Pd-decorated nanomaterials. In addition, an overview of the previous quantum chemical studies on the interactions between H_2 and such nanomaterials is presented.

2. Computational details

The adsorption of H_2 onto different nanomaterials was studied using DFT. The Gaussian 16 program was used to conduct the DFT calculations (Frisch et al., 2016). All structures were optimized at the wB97XD/6-311G(d, p) level (Chai and Head-Gordon, 2008). For optimizing the palladium complexes, the LANL2DZ basis set is used for Pd. They were confirmed as energy minima through a vibrational frequency analysis. The adsorption energy of the pollutant molecule on the nanocage (E_{ads}) is computed as follows:

$$E_{ads} = E_{H_2/nanomaterial} - (E_{nanomaterial} + E_{H_2}) + E_{BSSE} \quad (1)$$

where $E_{H_2/nanomaterial}$, $E_{nanomaterial}$, and E_{H_2} represent the energy of the H_2-adsorbed nanomaterial, the nanomaterial, and the H_2 molecule, respectively. E_{BSSE} represents the basis set superposition error (BSSE) correction determined by the counterpoise method (Boys and Bernardi, 1970).

The Multiwfn software (Lu and Chen, 2012) was used to perform the Bader's quantum theory of atoms in molecules (QTAIM) analysis (Bader, 1991) at the wB97XD/6-311G(d, p) level. The various types of atomic interactions could be identified from the values of the electron density (ρ_b) and its Laplacian ($\nabla^2\rho_b$) and the total electron energy density (H_b) and its components (kinetic electron energy density (G_b) and potential electron energy density (V_b)) at the bond critical point (Ziółkowski et al., 2006). $\nabla^2\rho_b < 0$ usually represents a covalent interaction. $\nabla^2\rho_b > 0$ and $H_b > 0$ represent non-covalent interactions (e.g., electrostatic and van der Waals interactions). $\nabla^2\rho_b > 0$ and $H_b < 0$ represent partially covalent interactions. In addition, $-G_b/V_b < 0.5$, $0.5 < -G_b/V_b < 1$, and $-G_b/V_b > 1$ represent covalent, partially covalent, and noncovalent interactions, respectively.

3. Results and discussion

3.1 Nanosheets

3.1.1 Graphene nanosheet

In the current study, the results (Fig. 1) show that the adsorption distance of H_2 on nanosheets follows the order: Pd-decorated graphene (1.71 Å) < Li-decorated graphene (2.16 Å) < graphene (2.96 Å) < Ca-decorated graphene (4.78 Å). The E_{ads} values for the adsorption of H_2 on nanosheets follow the order: Pd-decorated graphene (-17.73 kcal/mol) < Li-decorated graphene (-5.18 kcal/mol) < graphene (-1.49 kcal/mol) < Ca-decorated graphene (-0.11 kcal/mol). We find that H_2 is relatively strongly adsorbed on Pd-decorated graphene. The molecular electrostatic potential (MESP) minimum (V_{min}) is the most negatively valued point, which predicts the sites of electron localization in a molecule (Suresh et al., 2022; Nair et al., 2024, 2025). An MESP analysis showed that the MESP V_{min} is located near the Pd atom of the Pd-decorated graphene, and the difference in the MESP V_{min} due to H_2 adsorption (ΔV_{min}) is -3.07 kcal/mol. This implies that the Pd-decorated graphene becomes electron-rich due to the adsorption process.

In addition, we provide an overview of the previous studies that investigated the graphene nanosheets for hydrogen storage. The experimentally determined adsorption energy of H_2 on graphite was about -1.0 kcal/mol (Mattera et al., 1980; Vidali et al., 1991). Rubeš et al. (2010) studied the physical adsorption of H_2 on a graphite substrate at the DFT/CC level of theory (Rubeš and Bludský, 2009). The adsorption distance and the adsorption energy for the H_2/coronene system were 3.07 Å and -1.20 kcal/mol, respectively. The corresponding values for the H_2/graphene system were 3.06 Å and -1.30 kcal/mol, respectively. Similar results were obtained by other theoretical studies (Yeamin et al., 2014; de Lara-Castells and Mitrushchenkov, 2015; Bartolomei et al., 2017; Petrushenko and Petrushenko, 2019). Though different DFT methods present somewhat different adsorption energies, they arrive at the same trend for hydrogen storage.

Experimental studies have shown that the decoration of graphene nanosheets with metals can be used to tune the H_2 uptake process (Wang et al., 2025). Experimental studies also

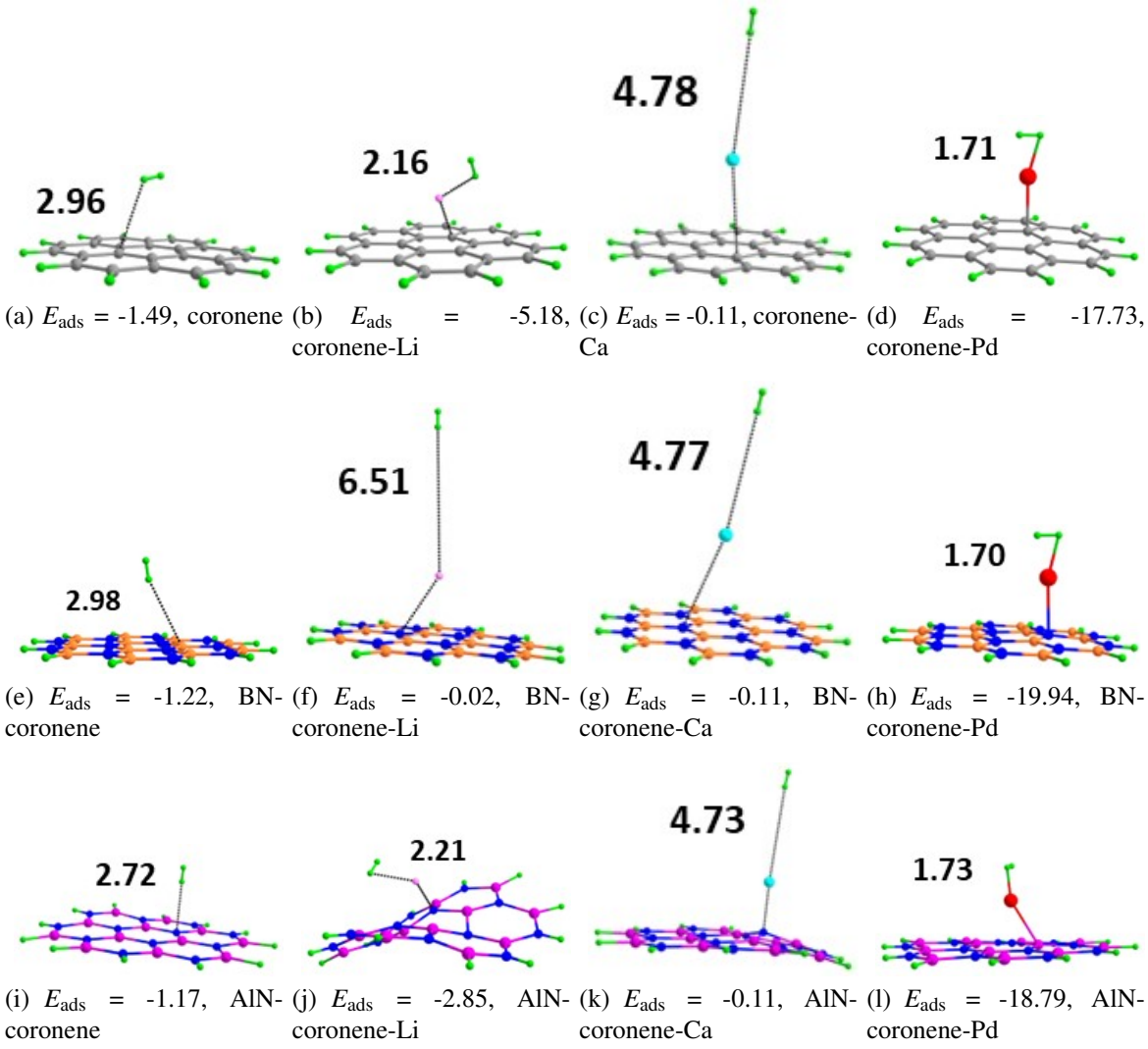

(a) E_{ads} = -1.49, coronene (b) E_{ads} = -5.18, coronene-Li (c) E_{ads} = -0.11, coronene-Ca (d) E_{ads} = -17.73, coronene-Pd

(e) E_{ads} = -1.22, BN-coronene (f) E_{ads} = -0.02, BN-coronene-Li (g) E_{ads} = -0.11, BN-coronene-Ca (h) E_{ads} = -19.94, BN-coronene-Pd

(i) E_{ads} = -1.17, AlN-coronene (j) E_{ads} = -2.85, AlN-coronene-Li (k) E_{ads} = -0.11, AlN-coronene-Ca (l) E_{ads} = -18.79, AlN-coronene-Pd

Fig. 1. Optimized structures of H_2 adsorbed on nanosheets. The adsorption distance and E_{ads} are given in Å and kcal/mol, respectively. Color code: Grey-C, green-H, orange-B, purple-Al, blue-N, pink-Li, cyan-Ca, red-Pd.

showed a high hydrogen storage capacity for Pd-decorated N-doped graphene (Parambhath and Ramaprabhu, 2012). Theoretical studies showed that the maximum number of H_2 adsorbed on the Li atom in decorated graphene was counted to be four (Ataca et al., 2008; Zheng et al., 2020). Each of the adsorbed Ca atoms on the graphene could bind up to five H_2 molecules (Ataca et al., 2021). It was found that the physisorption of H_2 is greatly enhanced by doping Al into graphene (Ao et al., 2009; Ao and Peeters, 2010). The E_{ads} values of H_2 on transition metal-doped graphene nanosheet increased from Sc to Ni, except for Cr. (Valencia and Frapper, 2015) Graphene decorated with Sc, Ti, Co, and Fe were good candidates for H_2 storage (Valencia and Frapper, 2015). Ti, Sc, and V atoms adsorbed on graphene can bind up to four hydrogen molecules (Durgun et al., 2008). H_2 adsorbed with Cu- and Pd-decorated defective graphene with an energy in range of -6.0 to -10.4 kcal/mol (Choudhary et al., 2016). The E_{ads} value reported by Choudhary et al. (2016) for the adsorption of H_2 on Pd-decorated graphene is consistent with our results. The syntheses of B and/or N substituted graphene have been achieved (Wei et al., 2009; Beheshti et al., 2011; Chang et al., 2013; Wang et al., 2014). The adsorption distance and E_{ads} value reported by Beheshti et al. (2011) for the adsorption of H_2 on Ca-decorated coronene are consistent with our results. Up to four H_2 can stably bind to a Ca atom on a graphene with substitutional doping of a single boron atom (Beheshti et al., 2011). The adsorption energy of H_2 on the decorated Sc and Cu atoms enhanced with increasing N-concentration on defective graphene (Luo et al., 2017; Singla and Jaggi, 2021). A crossover between multipole Coulomb and Kubas interactions was found for H_2 adsorption on alkaline-earth metal dispersed in B-doped graphenes (Kim et al., 2009). H_2 molecules dissociated on interaction with transition metal decorated B-doped graphene (Nachimuthu et al., 2014). The BC_3 and C_3N nanosheets have been experimentally synthesized (Aydin and Şimşek, 2019; Faye et al., 2019). DFT studies showed that the binding of H_2 on Li/Na/Mg-decorated BC_3 nanosheet comes from not only

the polarization mechanism but also the orbital hybridizations (Aydin and Şimşek, 2019). The binding properties of H_2 on C_3N could be enhanced considerably by suitable Sc and Ti doping (Faye et al., 2019). Several reviews have appeared that highlights various aspects of this area of research (Shevlin and Guo, 2009; Spyrou et al., 2013; Chung et al., 2015; Shiraz and Tavakoli, 2017; Singla and Jaggi, 2021; Cruz-Martínez et al., 2024).

3.1.2 h-BN nanosheet

In the current study, the results (Fig. 1) show that the adsorption distance of H_2 on nanosheets follows the order: Pd-decorated h-BN nanosheet (1.70 Å) < h-BN nanosheet (2.98 Å) < Ca-decorated h-BN nanosheet (4.77 Å) < Li-decorated h-BN nanosheet (6.51 Å). The E_{ads} values for the adsorption of H_2 on nanosheets follow the order: Pd-decorated h-BN nanosheet (-19.94 kcal/mol) < h-BN nanosheet (-1.22 kcal/mol) < Ca-decorated h-BN nanosheet (-0.11 kcal/mol) < Li-decorated h-BN nanosheet (-0.02 kcal/mol). We find that H_2 is relatively strongly adsorbed on Pd-decorated h-BN nanosheet.

Furthermore, experimental studies have shown that pristine and O-doped BN-nanosheets exhibits an excellent performance in hydrogen storage (Lei et al., 2014). DFT studies showed that the adsorption energy for H_2 adsorption on the BN-nanosheet (-0.87 kcal/mol) was similar to that of the graphene nanosheet (-0.98 kcal/mol) (Petrushenko and Petrushenko, 2019). The adsorption energy for H_2 adsorption on the BN-nanosheet was about 1.50 kcal/mol with GGA-PBE and 3.23 kcal/mol with LDA (Lei et al., 2014). The H_2 storage capacity of BN-nanosheets was enhanced by oxygen doping. Chettri et al. reported that the adsorption distance and the adsorption energy for the H_2/BN-nanosheet system were 3.02 Å and -4.89 kcal/mol, respectively (Chettrio et al., 2021). The H-H bond length changed from 0.74 Å to only 0.78 Å due to adsorption. The adsorption energy decreased with an increase in the number of adsorbed H_2 molecules. The adsorption energy was -2.95 kcal/mol per H_2 for the maximum hydrogen storage capacity (Chettrio et al., 2021). The adsorption of H_2 on BN nanosheet was endothermic with respect to dissociation (Wu et al., 2006; Shevlin and Guo, 2007).

The E_{ads} of H_2 on superalkali OLi_3-decorated BN-nanosheet was -4.7 kcal/mol (Zhang et al., 2023). This was attributed to the weak orbital interaction and electrostatic mutual attraction between the H atom and Li atom. A similar E_{ads} value was obtained for the superalkali NLi_4-decorated BN nanosheet (Wang et al., 2021).The adsorption energy of H_2 on C and O co-doped BN-nanosheet was higher than that on C- and O-doped BN-nanosheet (Kumar et al., 2015). The first H_2 molecule was adsorbed dissociatively over Rh atom, and molecularly on Ni decorated BN nanosheet (Venkataramanan et al., 2009). Three H_2 molecules were bound on the Ni-decorated defective BN nanosheet (Zhou et al., 2018). Co- and Pt-decorated C-doped BN nanosheet enhanced the H_2 storage performances (Aal and Alfuhaidi, 2021). For alkali metal-decorated defective BN nanosheet, there were up to four, six, and six H_2 molecules adsorbed on each Li, Na, and K, respectively, with the average adsorption energy in the range of -3.6 to -5.6 kcal/mol (Wang et al., 2022). The polarization mechanism and orbital hybridization were involved in H_2 adsorption on Ca-decorated defective BN nanosheets (Ma et al., 2021). The C-doped BN nanosheet eliminated the Ti-cluster, hence the capacity of H_2 storage was enhanced (Wang et al., 2022).

3.1.3 h-AlN nanosheet

In the current study, the results (Fig. 1) show that the adsorption distance of H_2 on nanosheets follows the order: Pd-decorated h-AlN nanosheet (1.73 Å) < Li-decorated h-AlN nanosheet (2.21 Å) < h-AlN nanosheet (2.72 Å) < Ca-decorated h-AlN nanosheet (4.73 Å). The E_{ads} values for the adsorption of H_2 on nanosheets follow the order: Pd-decorated h-AlN nanosheet (-18.79 kcal/mol) < Li-decorated h-AlN nanosheet (-2.85 kcal/mol) < h-AlN nanosheet (-1.17 kcal/mol) < Ca-decorated h-AlN nanosheet (-0.11 kcal/mol). We find that H_2 is relatively strongly adsorbed on Pd-decorated h-AlN nanosheet.

h-AlN nanosheets have been fabricated, for example, on Si substrates (Zhang et al., 2007; Tsipas et al., 2013). Moradi and Naderi (2014) found H_2 to be adsorbed collinearly on an N atom of the h-AlN nanosheet, which is consistent with our results.

3.2 Nanotubes

3.2.1 CNT

In the current study, the results (Fig. 2) show that the adsorption distance of H_2 on nanotubes follows the order: Pd-decorated CNT (1.75 Å) < Li-decorated CNT (2.13 Å) < Ca-decorated CNT (2.44 Å) < CNT (2.88 Å). The E_{ads} values for the adsorption of H_2 on nanotubes follow the order: Pd-decorated CNT (-14.71 kcal/mol) < Ca-decorated CNT (-5.05 kcal/mol) < Li-decorated CNT (-3.87 kcal/mol) < CNT (-1.38 kcal/mol). We find that H_2 is relatively strongly adsorbed on Pd-decorated CNT.

The experimentally determined adsorption energy of H_2 on some SWCNT bundles (-1.20 to -1.43 kcal/mol was similar to that on graphite (Schimmel et al., 2003; Brown et al., 2000). Rubeš and Bludský (2009) predicted that an H_2 molecule is mostly stabilized inside the (10,10)-CNT with an estimated adsorption energy of -1.72 kcal/mol at the DFT/CC level of theory. A similar value (-1.37 kcal/mol) was reported for (10, 0)-CNT by Han and Lee (2004). The adsorption energies of H_2 on (10, 0) (diameter of 7.8 Å), (5, 5) (diameter of 6.8 Å), and (17, 0) (diameter of 13.3 Å) CNTs were predicted to be -2.61, -1.92, and -1.13 kcal/mol, respectively (Zhao et al., 2002).

The syntheses of B and/or N substituted CNTs have been achieved (Sawant et al., 2022). The E_{ads} value of H_2 on (8, 0) CNT was -2.5 kcal/mol (Zhou et al., 2006). However, in the B or N-doped (8, 0) CNT when H_2 is adsorbed on top of B or N atom, the adsorption energies are the lowest (Zhou et al., 2006). The hydrogen storage properties of CNTs can be tuned by decoration with metals (Lyu et al., 2020). The E_{ads} value (per H_2) of H_2 on Ca-decorated B-doped (9, 0) CNT was -3.0 kcal/mol (Kim et al., 2009). BC_3 nanotubes have

been experimentally synthesized and DFT studies showed that lithiation of BC_3 nanotubes improved the performance of H_2 storage (Zhou et al., 2011). By increasing the coverage of H_2, the adsorption energy decreased for C_3N nanotubes (Eslami et al., 2016). The H_2 adsorption energy (per H_2) of the eight-Li-doped CNT was -4.0 kcal/mol, close to the lowest requirement (-4.6 kcal/mol) proposed by US DOE (Liu et al., 2009). For Ca-decorated CNTs, up to six H_2 molecules can bind to a Ca atom each with an adsorption energy of 3.9 kcal/mol (Lee et al., 2009). Single Al atom-decorated on (8, 0) CNT adsorbed up to six H_2 molecules with an adsorption energy (per H_2) of -4.6 kcal/mol (Seenithurai et al., 2014). Each Ti atom adsorbed on a CNT can bind up to four hydrogen molecules, one of which is dissociated (Yildirim and Ciraci, 2005). Sc and V atoms adsorbed on a CNT can bind up to five hydrogen molecules (Durgun et al., 2008). The E_{ads} values of H_2 on transition metal-doped (8, 0) CNTs increased from Sc to Ni, except for Cr (Valencia and Frapper, 2015). The Sc atoms clustering on CNTs with diameters 1-2 nm, is energetically favorable and kinetically permitted (Krasnov et al., 2007). The Y-decorated CNT has also the potential to become a promising hydrogen storage device (Chakraborty et al., 2012).

3.2.2 BNNT

In the current study, the results (Fig. 2) show that the adsorption distance of H_2 on nanotubes follows the order: Pd-decorated BNNT (1.71 Å) < BNNT (2.79 Å) < Ca-decorated BNNT (4.79 Å) < Li-decorated BNNT (6.42 Å). The E_{ads} values for the adsorption of H_2 on nanosheets follow the order: Pd-decorated BNNT (-20.05 kcal/mol) < BNNT (-1.30 kcal/mol) < Ca-decorated BNNT (-0.12 kcal/mol) < Li-decorated BNNT (-0.01 kcal/mol). We find that H_2 is relatively strongly adsorbed on Pd-decorated BNNT.

Experimental studies have shown that BNNTs can be explored as a possible hydrogen storage medium (Ma et al., 2002; Tang et al., 2002). DFT studies showed that the ionic character of the BN bonds in BNNTs is the key point that increases the binding energy of H_2 (Mpourmpakis and Froudakis, 2007). The E_{ads} value of H_2 on (10, 0) BNNT (-2.5 kcal/mol) was more negative than that on BN-nanosheet (-2.1 kcal/mol) (Jhi and Kwon, 2004). The adsorption of H_2 on BNNT was endothermic with respect to dissociation, with the small-diameter nanotube possessing the smaller barrier (Wu et al., 2006; Shevlin and Guo, 2007). Durgun et al. showed that the interaction of H_2 with (8, 0) BNNT is very weak (Durgun et al., 2007). However, BNNT can be functionalized by Ti atom and single Ti can bind up to four H_2 molecules, one is dissociated and the remaining three are molecularly absorbed. Seven H_2 molecules can bind with the Ce-doped BNNT system with average adsorption energy of -6.5 kcal/mol (Zhang et al., 2012). H_2 adsorption energies on C-doped BNNTs were enhanced when compared with clean BNNTs (Baierle et al., 2006). It was found that single Rh, Ni, and Pd adsorbed on BNNT can bind up to four, three, and two H_2 molecules, respectively, accompanied by a significant elongation of H-H bonds (Zhang et al., 2011). The E_{ads} value of H_2 on Al-doped (3, 3) BNNT (diameter of 4.1 Å) was -6.0 kcal/mol (Noura et al., 2020). The intramolecular H_2 bond length increased from the equilibrium length of 0.74 Å to 0.787 Å in the presence of Mg-doped BNNT (Noura et al., 2023). Na and K decorated BNNTs can store up to seven H_2 molecules each, while Li can only accommodate six H_2 molecules around it (Satawara et al., 2024). Metal-doped BNNTs with B/N/BN defects can also improve the hydrogen storage (Mananghaya and Santos, 2016; Ma et al., 2021).

3.2.3 AlNNT

In the current study, the results (Fig. 2) show that the adsorption distance of H_2 on nanotubes follows the order: Pd-decorated AlNNT (1.71 Å) < Li-decorated AlNNT (2.19 Å) < AlNNT (2.62 Å) < Ca-decorated AlNNT (4.80 Å). The E_{ads} values for the adsorption of H_2 on nanosheets follow the order: Pd-decorated AlNNT (-20.09 kcal/mol) < Li-decorated AlNNT (-2.30 kcal/mol) < AlNNT (-1.55 kcal/mol) < Ca-decorated AlNNT (-0.11 kcal/mol). We find that H_2 is relatively strongly adsorbed on Pd-decorated AlNNT.

Experimentally, AlNNTs have been synthesized using various methods (Tondare et al., 2002; Wu et al., 2003). DFT studies showed that the adsorption configuration of H_2 adsorbed on the Al atom of the AlNNT was the most energetically favorable (Kuang et al., 2021). When H_2 molecules were adsorbed on the outer surface of the AlNNT, the E_{ads} value remained essentially unchanged (Wang et al., 2009). Enhanced adsorption of H_2 was found on Au- and Ag-decorated AlNNT (Eno et al., 2023).

3.3 Nanocages

3.3.1 Carbon fullerene and its fragments

In the current study, the results (Fig. 3) show that the adsorption distance of H_2 on C_{60} fullerene follows the order: Pd-decorated C_{60} fullerene (1.81 Å) < Li-decorated C_{60} fullerene (2.10 Å) < Ca-decorated C_{60} fullerene (2.37 Å) < C_{60} fullerene (3.10 Å). The E_{ads} values for the adsorption of H_2 on nanosheets follow the order: Pd-decorated C_{60} fullerene (-20.68 kcal/mol) < Li-decorated C_{60} fullerene (-4.30 kcal/mol) < Ca-decorated C_{60} fullerene (-4.22 kcal/mol) < C_{60} fullerene (-1.11 kcal/mol). We find that H_2 is relatively strongly adsorbed on Pd-decorated C_{60} fullerene. Generally similar trends are observed for the corresponding corannulene and sumanene systems (see Fig. 3).

Experimental studies showed that alkaline earth metals such as Ca and Sr can be stabilized on C_{60} (Zimmermann et al., 1994). DFT studies showed that Ca or Sr coating of C_{60} results in strong H_2 binding sites (Yoon et al., 2008). Also, the doping of alkali metal atoms on C_{60} enhanced H_2 adsorption (Chandrakumar and Ghosh, 2008). Transition metal atoms bound to C_{60} and $C_{48}B_{12}$ fullerenes were proposed as adsorbents for high density, room temperature, ambient pressure storage of H_2 (Zhao et al., 2005). The Kubas-type (or orbital) interaction between H_2 and transition metal can lead to significant adsorption energy (Hoang and Antonelli, 2009). However, transition metal atoms such as Ti would prefer to cluster on the C_{60} surface, which can reduce the weight percentage of H_2 storage (Sun et al., 2005). The synthesis of the smallest possible fullerene C_{20} was reported in the year 2000

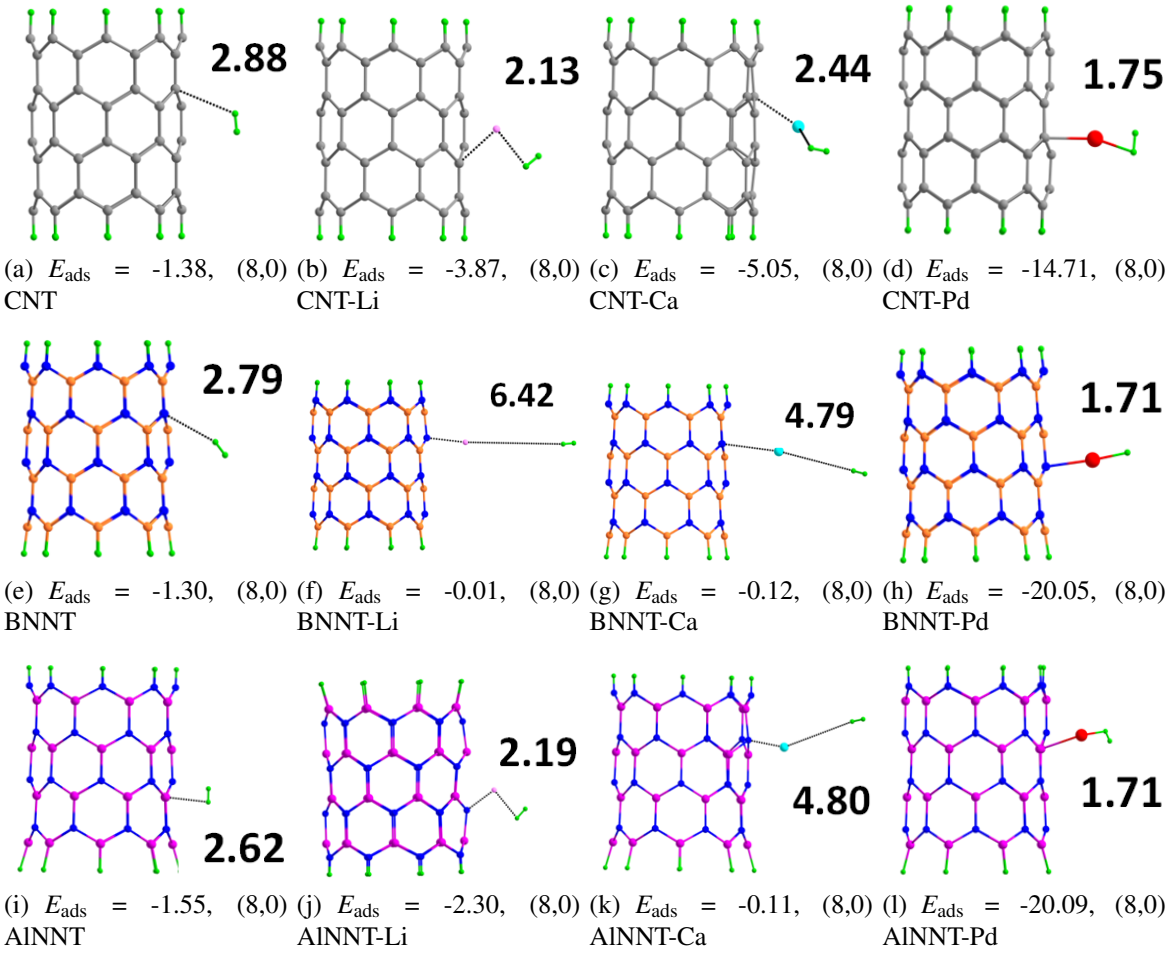

(a) E_{ads} = -1.38, (8,0) CNT (b) E_{ads} = -3.87, (8,0) CNT-Li (c) E_{ads} = -5.05, (8,0) CNT-Ca (d) E_{ads} = -14.71, (8,0) CNT-Pd

(e) E_{ads} = -1.30, (8,0) BNNT (f) E_{ads} = -0.01, (8,0) BNNT-Li (g) E_{ads} = -0.12, (8,0) BNNT-Ca (h) E_{ads} = -20.05, (8,0) BNNT-Pd

(i) E_{ads} = -1.55, (8,0) AlNNT (j) E_{ads} = -2.30, (8,0) AlNNT-Li (k) E_{ads} = -0.11, (8,0) AlNNT-Ca (l) E_{ads} = -20.09, (8,0) AlNNT-Pd

Fig. 2. Optimized structures of H_2 adsorbed on nanotubes. The adsorption distance and E_{ads} are given in Å and kcal/mol, respectively. Color code: Grey-C, green-H, orange-B, purple-Al, blue-N, pink-Li, cyan-Ca, red-Pd.

(Prinzbach et al., 2000). The E_{ads} value (per H_2 molecule) for the adsorption of H_2 on alkali metal-decorated C_{20} was -2.9 kcal/mol (Sahoo et al., 2021). There are experimental reports that fullerene cage molecules can be doped with heteroatoms such as B and/or N atoms (Guo et al., 1991; Pradeep et al., 1991; Nakamura et al., 1999; Hultman et al., 2001; Otero et al., 2008). Using DFT Kim et al. studied the adsorption of H_2 on, for example, N- and B-doped fullerenes (Kim et al., 2006). They found that the adsorption energy for the adsorption of H_2 on $C_{35}B$ fullerene was higher than that on $C_{35}N$ fullerene.

Li atoms in $Li_{12}C_{48}B_{12}$ heterofullerene, like that in $Li_{12}C_{60}$, do not cluster and the E_{ads} value for the adsorption of H_2 on $Li_{12}C_{48}B_{12}$ was -4.0 kcal/mol (Sun et al., 2009). Unlike $C_{60}Ca_x$ fullerene (with x = 1-6), $C_{48}B_{12}Ca_x$ fullerene was stable with respect to decomposition into the fullerene molecules and Ca bulk metal (Er et al., 2015). The E_{ads} value (per H_2 molecule) for the adsorption of H_2 on transition metal decorated $C_{24}N_{24}$ ($C_{24}N_2-V_6(H_2)_6$) was -8.9 kcal/mol (Srinivasu and Ghosh, 2012). The E_{ads} value for the adsorption of H_2 on charged fullerenes can be enhanced to -7.4 kcal/mol (Yoon et al., 2007). Experimental studies showed that H_2 can also be encapsulated in a fullerene cage (Komatsu et al., 2005). The structures with a large amount of encapsulated H_2 were highly endothermic (Pupysheva et al., 2008).

Experimental studies showed that H_2 adsorption on corannulene occurred via weak van der Waals interactions following a type-V isotherm (Gaboardi et al., 2019). DFT studies showed that the E_{ads} values of H_2 on corannulene and N-doped corannulene were -2.4 and -2.9 kcal/mol, respectively (Denis, 2008). The doping of lithium atoms to corannulene systems improved the H_2 adsorption (Zhang et al., 2006). Sumanene possessed high H_2 binding affinity (Della and Suresh, 2018). The E_{ads} value of H_2 on sumanene was estimated as -3.7 kcal/mol. The synthesis of sumanenyl anions stabilized by K^+ has been reported by Spisak et al., 2015. The E_{ads} values (per H_2 molecule) for the adsorption of H_2 on the ion-pair complexes of anionic, dianionic, and trianionic sumanenes with K^+ were -1.3, -1.5 and -2.6 kcal/mol, respectively. The MESP analysis suggested strong charge separation in these ion pair systems, which promotes the binding of H_2 molecules (Della and Suresh, 2018). The modification of sumanene with N atoms favored H_2 adsorption, whereas an opposite trend was found with B atoms (Armaković et al., 2016).

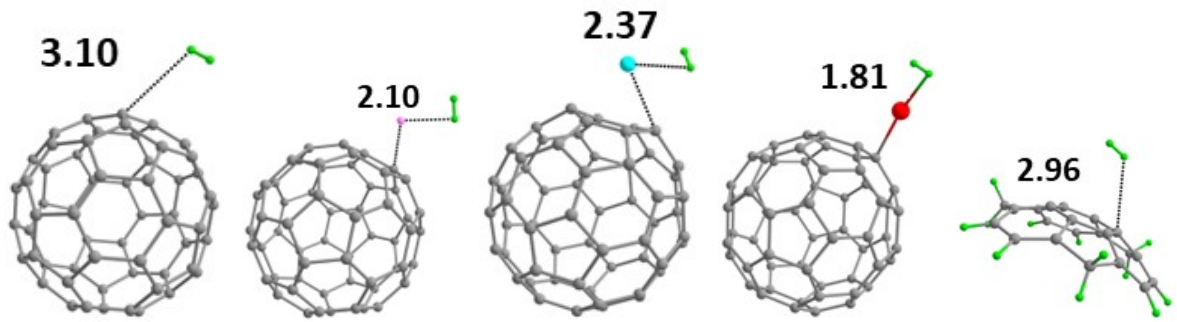

(a) E_{ads} = -1.11, C_{60} (b) E_{ads} = -4.30, C_{60}-Li (c) E_{ads} = -4.22, C_{60}-Ca (d) E_{ads} = -20.68, C_{60}-Pd (e) Sumanene, E_{ads} = -1.15

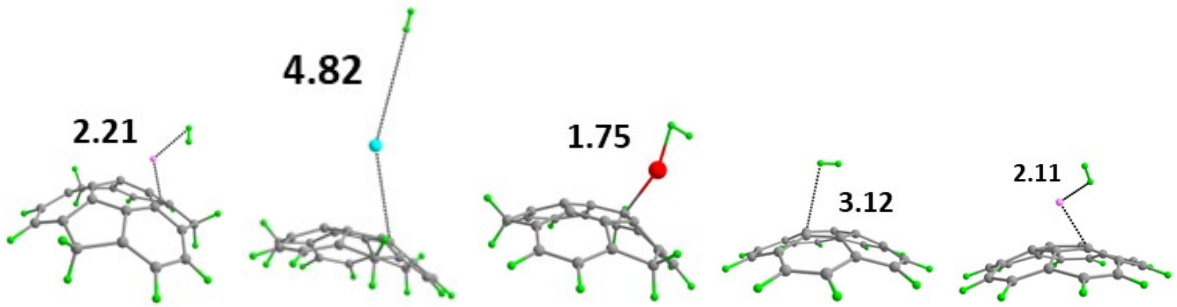

(f) Sumanene-Li, E_{ads} = -3.90 (g) Sumanene-Ca, E_{ads} = -0.12 (h) Sumanene-Pd, E_{ads} = -14.93 (i) E_{ads} = -0.98, corannulene (j) E_{ads} = -4.20, corannulene-Li

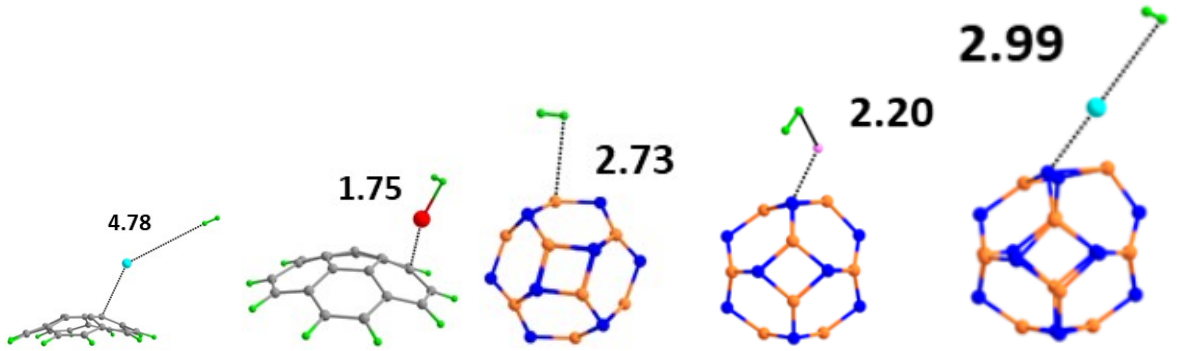

(k) E_{ads} = -0.75, corannulene-Ca (l) E_{ads} = -15.38, corannulene-Pd (m) E_{ads} = -0.94, $B_{12}N_{12}$ (n) E_{ads} = -3.41, $B_{12}N_{12}$-Li (o) E_{ads} = -1.10, $B_{12}N_{12}$-Ca

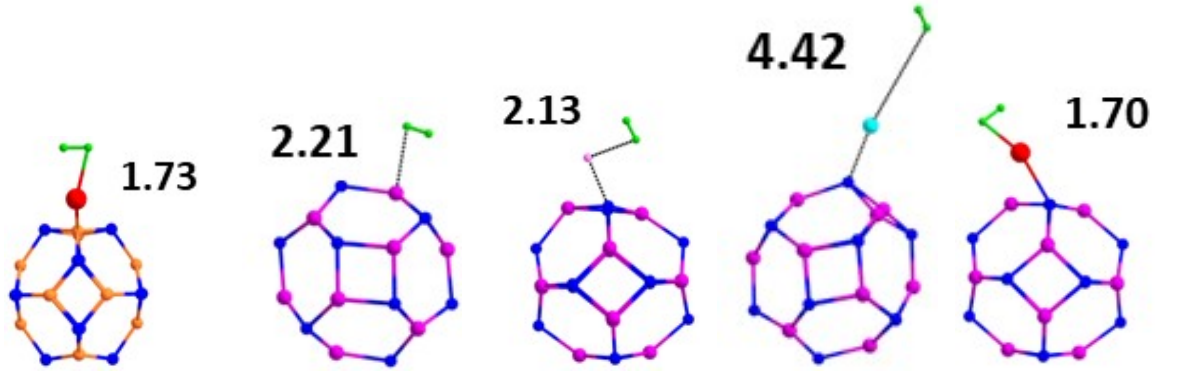

(p) E_{ads} = -18.74, $B_{12}N_{12}$-Pd (q) E_{ads} = -3.32, $Al_{12}N_{12}$ (r) E_{ads} = -2.75, $Al_{12}N_{12}$-Li (s) E_{ads} = -0.30, $Al_{12}N_{12}$-Ca (t) E_{ads} = -21.95, $Al_{12}N_{12}$-Pd

Fig. 3. Optimized structures of H_2 adsorbed on nanocages. The adsorption distance and E_{ads} are given in Å and kcal/mol, respectively. Color code: grey-C, green-H, orange-B, purple-Al, blue-N, pink-Li, cyan-Ca, red-Pd.

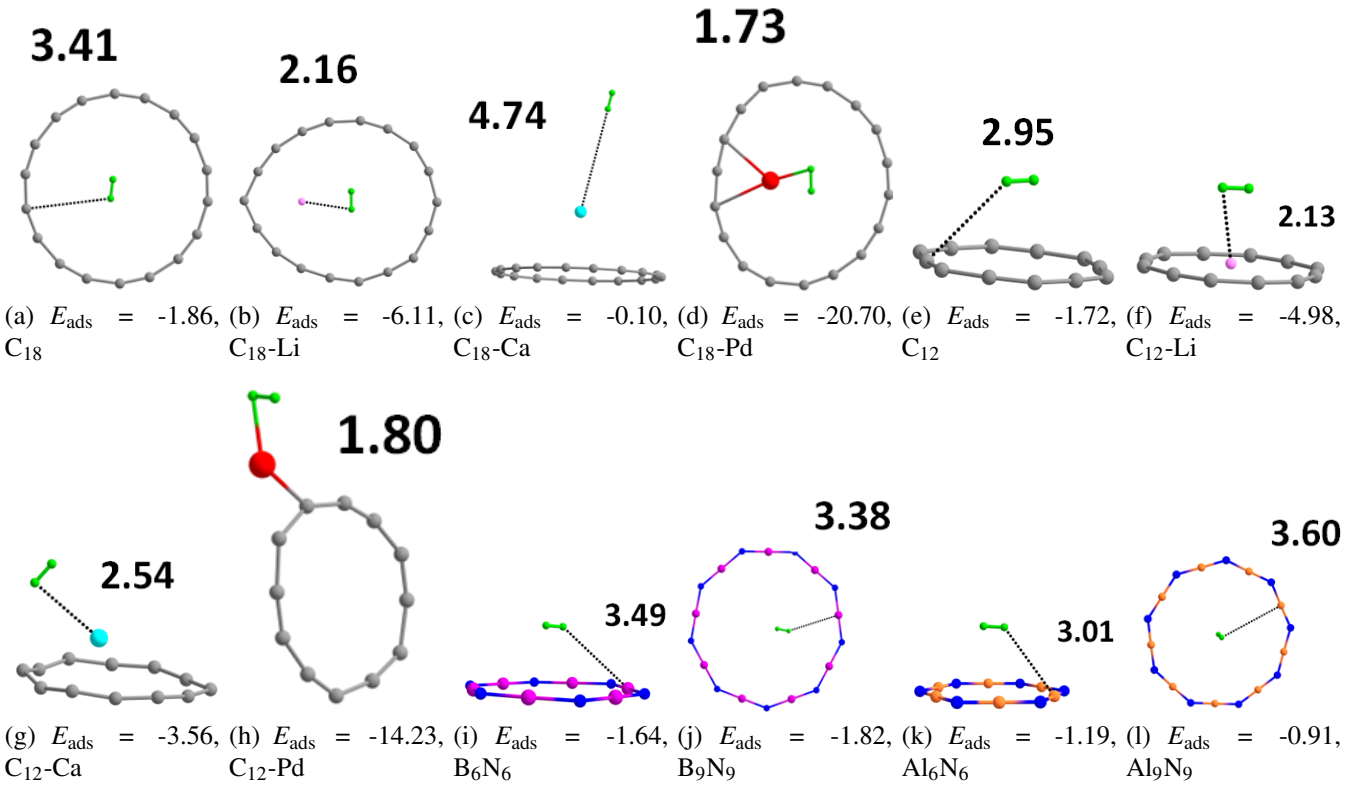

(a) E_{ads} = -1.86, C_{18} (b) E_{ads} = -6.11, C_{18}-Li (c) E_{ads} = -0.10, C_{18}-Ca (d) E_{ads} = -20.70, C_{18}-Pd (e) E_{ads} = -1.72, C_{12} (f) E_{ads} = -4.98, C_{12}-Li

(g) E_{ads} = -3.56, C_{12}-Ca (h) E_{ads} = -14.23, C_{12}-Pd (i) E_{ads} = -1.64, B_6N_6 (j) E_{ads} = -1.82, B_9N_9 (k) E_{ads} = -1.19, Al_6N_6 (l) E_{ads} = -0.91, Al_9N_9

Fig. 4. Optimized structures of H_2 adsorbed on nanorings. The adsorption distance and E_{ads} are given in Å and kcal/mol, respectively. Color code: Grey-C, green-H, orange-B, purple-Al, blue-N, pink-Li, cyan-Ca, red-Pd.

3.3.2 $B_{12}N_{12}$ and $Al_{12}N_{12}$ nanocages

Fig. 3 also shows the interaction of H_2 with pristine and metal-decorated $B_{12}N_{12}$ and $Al_{12}N_{12}$ nanocages. Our results show that H_2 is relatively strongly adsorbed on Pd-decorated $B_{12}N_{12}$ and $Al_{12}N_{12}$ nanocages.

Oku et al. synthesized and detected the $B_{12}N_{12}$ nanocage clusters using the laser desorption time-off-light mass spectrometry (Oku et al., 2004). Theoretical studies have shown that among AlnNn (n = 2-41) nanocages, $Al_{12}N_{12}$ is the most stable nanocage (Wu et al., 2003). Using DFT, we recently showed that the adsorption distance and the adsorption energy for the $H_2/B_{12}N_{12}$ system were 2.67 Å and -0.83 kcal/mol, respectively (Nair et al., 2024). The corresponding values for the $H_2/Al_{12}N_{12}$ system were 2.15 Å and -3.66 kcal/mol, respectively (Nair et al., 2024). The analysis of adsorption free energy showed that the adsorption of H_2 on the $B_{12}N_{12}$ and $Al_{12}N_{12}$ nanocages is endergonic, indicative of the weak interactions. The ΔV_{min} values for the $H_2/B_{12}N_{12}$ and $H_2/Al_{12}N_{12}$ systems were -0.56 and -6.53 kcal/mol, respectively. This implied that the $B_{12}N_{12}$ and $Al_{12}N_{12}$ nanocages become electron-rich due to the adsorption process. As H_2 molecules approach the positively charged Al of $Al_{12}N_{12}$, the charge on Al polarizes the electron clouds in H_2, inducing electrostatic interactions (Wang et al., 2009). Also, the low-lying unoccupied valence orbitals available in Al of $Al_{12}N_{12}$ mix with the σ bonding orbital of H_2, resulting in the donation of the σ electrons into the vacant orbitals of Al (Wang et al., 2009).

The H_2 adsorption had not much effect on the DFT reactivity indices (μ, η, s, and ω) of the $B_{12}N_{12}$ and $Al_{12}N_{12}$ nanocages (Nair et al., 2024). The quantum theory of atoms in molecules (QTAIM) analysis suggested the noncovalent nature of interactions in these systems. For instance, the ρ_b values of the $H_2/B_{12}N_{12}$ and $H_2/Al_{12}N_{12}$ systems were 0.007 and 0.020 a.u., respectively, and the corresponding $\nabla^2\rho_b$ values were positive. The non-covalent interaction (NCI) analysis indicated the presence of van der Waals interactions between H_2 and the nanocages (Nair et al., 2024). Janjua studied the encapsulation of inorganic $B_{12}N_{12}$ nanocages with alkaline earth metals for efficient hydrogen adsorption (Janjua, 2021). The interaction energies of $Be-B_{12}N_{12}$, $Mg-B_{12}N_{12}$, and $Ca-B_{12}N_{12}$ were found to be -85.11, 197.41, and 257.70 kcal/mol, respectively. The Be metal being small accurately fitted in the cavity and exhibited exothermic adsorption energy. The encapsulation of Be, Mg, and Ca metals in $B_{12}N_{12}$ caused a significant change in the HOMO-LUMO energy gap. The E_{ads} values for the H_2 adsorption followed the order: $Ca-B_{12}N_{12}$ (-10.67 kcal/mol) > $Mg-B_{12}N_{12}$ (-8.04 kcal/mol) > $Be-B_{12}N_{12}$ (-7.06 kcal/mol) > $B_{12}N_{12}$ (-0.25 kcal/mol).

Zhang et al. studied the feasibility of Ni-decorated $Al_{12}N_{12}$ nanocage for H_2 storage using DFT (Zhang et al., 2012). Ni atom of the $NiAl_{12}N_{12}$ cage was found to adsorb up to three H_2 molecules with the average adsorption energy of -16.3 kcal/mol. Both the polarization of the H_2 molecules and the hybridization of the Li-2p orbitals with the H-s orbitals

contributed to the H_2 adsorption on Li-decorated $Al_{12}N_{12}$ (Wang et al., 2014; Zhang et al., 2024).

3.4 Cyclo[n]carbon and its analogues

In the current study, the results (Fig. 4) show that the adsorption distance of H_2 on C_{18} nanoring follows the order: Pd-decorated C_{18} nanoring (1.73 Å) < Li-decorated C_{18} nanoring (2.16 Å) < C_{18} nanoring (3.41 Å) < Ca-decorated C_{18} nanoring (4.74 Å). The E_{ads} values for the adsorption of H_2 on nanosheets follow the order: Pd-decorated C_{18} nanoring (-20.70 kcal/mol) < Li-decorated C_{18} nanoring (-6.11 kcal/mol) < C_{18} nanoring (-1.86 kcal/mol) < Ca-decorated C_{18} nanoring (-0.10 kcal/mol). We find that H_2 is relatively strongly adsorbed on Pd-decorated C_{18} nanoring. An MESP analysis showed that the MESP V_{min} is located near the Pd atom of the Pd-decorated C_{18} nanoring, and the ΔV_{min} value is -3.58 kcal/mol. This implies that the Pd-decorated C_{18} nanoring becomes electron-rich due to the adsorption process. Generally similar trends are observed for the corresponding C_{12} nanoring systems. Furthermore, our results show that H_2 is physiosorbed on B_9N_9, Al_9N_9, B_6N_6, and Al_6N_6 nanorings (see Fig. 4).

In 2019, Kaiser et al. (2019) reported the synthesis and structural characterization of C_{18} nanoring. The high-resolution atomic force microscopy showed a polyynic structure of C_{18} nanoring with alternating triple and single bonds. The syntheses of other cyclo[n]carbons (n = 10, 12, 14, and 20) have also been reported (Sun et al., 2024). DFT studies showed that H_2 can fit inside the C_{18} nanoring (Domínguez-Gutiérrez et al., 2021; Trzesowska et al., 2023).

3.5 QTAIM analysis

The QTAIM results for the nanomaterial/H_2 system are provided in Table 1. For all the Pd-decorated nanomaterials, ρ_b is relatively high, $\nabla^2\rho_b > 0$, $H_b < 0$, and $0.5 < -G_b/V_b < 1$. These results imply a partial covalent character for the interaction of H_2 with Pd-decorated nanomaterials. Similar results are obtained for the $Al_{12}N_{12}$ nanocage except that ρ_b is relatively low ($\rho_b = 0.017$ a.u.). For all other cases, ρ_b is relatively low, $\nabla^2\rho_b > 0$, $H_b > 0$, and $-G_b/V_b > 1$. These results imply a noncovalent character for the interaction of H_2 with these nanomaterials.

4. Conclusions

We performed DFT studies to understand the interactions between H_2 and nanomaterials such as pristine and Li/Ca/Pd-decorated graphene, h-BN nanosheet, h-AlN nanosheet, CNT, BNNT, AlNNT, C_{60} fullerene, corannulene, sumanene, $B_{12}N_{12}$ nanocage, $Al_{12}N_{12}$ nanocage, C_{18} nanoring, C_{12} nanoring, etc. Our results showed that, in general, H_2 was weakly adsorbed on these nanomaterials. For example, the adsorption distance for H_2 on graphene nanosheet and h-BN nanosheet were 2.96 and 2.98 Å, respectively. The corresponding E_{ads} values were -1.49 and -1.22 kcal/mol, respectively. However, H_2 was strongly adsorbed on Pd-decorated nanomaterials. For example, the adsorption distance for H_2 on Pd-decorated (8, 0) CNT and (8, 0) BNNT were 1.75 and 1.71 Å, respectively. The corresponding E_{ads} values were -14.71 and -20.05 kcal/mol, respectively. Interestingly, the adsorption of H_2 on Li/Ca-decorated nanomaterials was often but not always enhanced. Among the studied systems, the lowest negative E_{ads} value was observed for the Li-decorated (8, 0) BNNT (-0.01 kcal/mol) and the highest for the Pd-decorated $Al_{12}N_{12}$ nanocage (-21.95 kcal/mol). The QTAIM analysis found a partial covalent character for the interaction of H_2 with all the Pd-decorated nanomaterials and the $Al_{12}N_{12}$ nanocage, and a noncovalent character for the interaction of H_2 with the other studied nanomaterials.

We also provided an overview of the previous quantum chemical studies on the interactions between H_2 and such nanomaterials. The Kubas-type (or orbital) interaction between H_2 and transition metal can enhance the adsorption of H_2 on transition metal-decorated nanomaterials. However, transition metal atoms might cluster on the surface of the nanomaterials, thus undermining their capability to store hydrogen. The E_{ads} values (per H_2) typically become less negative with an increase in the number of H_2 molecules adsorbed. The interaction between H_2 and such metal-decorated nanomaterials can be tuned by replacing the C/B/Al/N atoms with heteroatoms and by introducing vacancy defects. These processes can ease the clustering problem of metals on the surface of the nanomaterials. These findings might provide strategies that use different dimensional nanomaterials decorated with metal atoms to effectively store hydrogen.

Acknowledgements

This publication is based upon work supported by the King Abdullah University of Science and Technology (KAUST) Office of Sponsored Research (OSR) under Award No. ORFS-2022-CRG11-5028 and BAS/1/1423-01-01. R. G. S. N. and A. K. N. N. would like to thank KAUST for providing computational resources for the Shaheen III supercomputer.

Conflict of interest

The authors declare no competing interest.

References

Ataca, C., Aktürk, E., Ciraci, S. A. L. I. M., et al. High-capacity hydrogen storage by metallized graphene. Applied Physics Letters, 2008, 93(4).

Ataca, C., Aktürk, E., Ciraci, S. Hydrogen storage of calcium atoms adsorbed on graphene: First-principles plane wave calculations. Physical Review B, 2009, 79: 041406.

Ao, Z. M., Jiang, Q., Zhang, R., et al. Al doped graphene: a promising material for hydrogen storage at room temperature. Journal of Applied Physics, 2009, 105(7).

Ao, Z. M., Peeters, F. M. High-capacity hydrogen storage in Al-adsorbed graphene. Physical Review B-Condensed Matter and Materials Physics, 2010, 81(20): 205406.

Aydin, S., Şimşek, M. The enhancement of hydrogen storage capacity in Li, Na and Mg-decorated BC_3 graphene by

Table 1. The QTAIM parameters (a.u.) for the nanomaterials interacting with H_2.

Nanomaterials	ρ_b	$\nabla^2\rho_b$	H_b	G_b	V_b	$-G_b/V_b$
Nanosheets						
coronene	0.005	0.016	0.001	0.003	-0.002	1.309
coronene-Li	0.009	0.047	0.002	0.009	-0.007	1.323
coronene-Ca	0.001	0.001	0.000	0.000	0.000	1.574
coronene-Pd	0.105	0.373	-0.039	0.132	-0.170	0.774
BN-coronene	0.005	0.014	0.001	0.003	-0.002	1.294
BN-coronene-Li	0.000	0.000	0.000	0.000	0.000	2.215
BN-coronene-Ca	0.001	0.001	0.000	0.000	0.000	1.603
BN-coronene-Pd	0.110	0.372	-0.042	0.135	-0.178	0.762
AlN-coronene	0.009	0.021	0.001	0.005	-0.004	1.133
AlN-coronene-Li	0.007	0.041	0.002	0.008	-0.006	1.426
AlN-coronene-Ca	0.001	0.001	0.000	0.000	0.000	1.502
AlN-coronene-Pd	0.102	0.383	-0.035	0.131	-0.166	0.789
Nanotubes						
(8,0) CNT	0.006	0.017	0.001	0.003	-0.003	1.296
(8,0) CNT-Li	0.009	0.049	0.002	0.010	-0.007	1.329
(8,0) CNT-Ca	0.016	0.072	0.003	0.015	-0.012	1.255
(8,0) CNT-Pd	0.096	0.360	-0.032	0.122	-0.153	0.793
(8,0) BNNT	0.006	0.017	0.001	0.004	-0.003	1.204
(8,0) BNNT-Li	0.000	0.000	0.000	0.000	0.000	2.159
(8,0) BNNT-Ca	0.001	0.001	0.000	0.000	0.000	1.599
(8,0) BNNT-Pd	0.107	0.376	-0.040	0.134	-0.175	0.769
(8,0) AlNNT	0.009	0.018	0.000	0.004	-0.004	1.063
(8,0) AlNNT-Li	0.007	0.044	0.003	0.008	-0.006	1.437
(8,0) AlNNT-Ca	0.001	0.001	0.000	0.000	0.000	1.562
(8,0) AlNNT-Pd	0.104	0.390	-0.036	0.134	-0.170	0.787
Nanocages						
C_{60}	0.004	0.013	0.001	0.003	-0.002	1.379
C_{60}-Li	0.009	0.052	0.003	0.010	-0.008	1.331
C_{60}-Ca	0.018	0.078	0.003	0.017	-0.014	1.205
C_{60}-Pd	0.084	0.329	-0.024	0.106	-0.129	0.818
sumanene	0.005	0.015	0.001	0.003	-0.002	1.319
sumanene-Li	0.009	0.050	0.002	0.010	-0.007	1.333
sumanene-Ca	0.001	0.001	0.000	0.000	0.000	1.617
sumanene-Pd	0.098	0.351	-0.034	0.121	-0.155	0.783
corannulene	0.004	0.014	0.001	0.003	-0.002	1.372
corannulene-Li	0.009	0.050	0.002	0.010	-0.008	1.324
corannulene-Ca	0.001	0.001	0.000	0.000	0.000	1.579
corannulene-Pd	0.098	0.356	-0.034	0.123	-0.156	0.785

Nanomaterials	ρ_b	$\nabla^2\rho_b$	H_b	G_b	V_b	$-G_b/V_b$
$B_{12}N_{12}$	0.006	0.019	0.001	0.004	-0.003	1.307
$B_{12}N_{12}$-Li	0.009	0.048	0.003	0.010	-0.007	1.368
$B_{12}N_{12}$-Ca	0.005	0.018	0.001	0.003	-0.003	1.354
$B_{12}N_{12}$-Pd	0.102	0.376	-0.035	0.129	-0.165	0.785
$Al_{12}N_{12}$	0.017	0.051	-0.000	0.013	-0.014	0.968
$Al_{12}N_{12}$-Li	0.008	0.046	0.002	0.009	-0.006	1.391
$Al_{12}N_{12}$-Ca	0.001	0.001	0.000	0.000	0.000	1.202
$Al_{12}N_{12}$-Pd	0.107	0.402	-0.038	0.139	-0.177	0.783
Cyclo[n]carbon and its analogues						
C_{18}	0.003	0.008	0.000	0.002	-0.001	1.276
C_{18}-Li	0.009	0.048	0.003	0.009	-0.007	1.369
C_{18}-Ca	0.001	0.001	0.000	0.000	0.000	1.613
C_{18}-Pd	0.101	0.375	-0.035	0.129	-0.165	0.785
C_{12}	0.004	0.014	0.001	0.003	-0.002	1.293
C_{12}-Li	0.009	0.055	0.003	0.011	-0.008	1.356
C_{12}-Ca	0.012	0.050	0.002	0.010	-0.008	1.275
C_{12}-Pd	0.086	0.350	-0.024	0.111	-0.135	0.824
B_6N_6	0.004	0.013	0.001	0.003	-0.002	1.452
B_9N_9	0.002	0.006	0.000	0.001	-0.001	1.859
Al_6N_6	0.002	0.006	0.000	0.001	-0.001	1.493
Al_9N_9	0.003	0.008	0.000	0.001	-0.001	1.420

CLICH and RICH algorithms. International Journal of Hydrogen Energy, 2019, 44(14): 7354-7370.

Aal, S. A., Alfuhaidi, A. K. Enhancement of hydrogen storage capacities of Co and Pt functionalized h-BN nanosheet: Theoretical study. Vacuum, 2021, 183: 109838.

Armaković, S., Armaković, S. J., Pelemiš, S., et al. Influence of sumanene modifications with boron and nitrogen atoms to its hydrogen adsorption properties. Physical Chemistry Chemical Physics, 2016, 18(4): 2859-2870.

Bartolomei, M., de Tudela, R. P., Arteaga, K., et al. Adsorption of molecular hydrogen on coronene with a new potential energy surface. Physical Chemistry Chemical Physics, 2017, 19(38): 26358-26368.

Beheshti, E., Nojeh, A., Servati, P. A first-principles study of calcium-decorated, boron-doped graphene for high capacity hydrogen storage. Carbon, 2011, 49(5): 1561-1567.

Brown, C. M., Yildirim, T., Neumann, D. A., et al. Quantum rotation of hydrogen in single-wall carbon nanotubes. Chemical Physics Letters, 2000, 329(3-4): 311-316.

Boys, S. F., Bernardi, F. J. M. P. The calculation of small molecular interactions by the differences of separate total energies. Some procedures with reduced errors. Molecular Physics, 1970, 19(4): 553-566.

Bader, R. F. A quantum theory of molecular structure and its applications. Chemical Reviews, 1991, 91(5): 893-928.

Baierle, R. J., Piquini, P., Schmidt, T. M., et al. Hydrogen adsorption on carbon-doped boron nitride nanotube. The Journal of Physical Chemistry B, 2006, 110(42): 21184-21188.

Chang, C., Kataria, S., Kuo, C., et al. Band gap engineering of chemical vapor deposited graphene by in situ BN doping. Acs Nano, 2013, 7(2): 1333-1341.

Chettri, B., Patra, P. K., Hieu, N. N., et al. Hexagonal boron nitride (h-BN) nanosheet as a potential hydrogen adsorption material: A density functional theory (DFT) study. Surfaces and Interfaces, 2021, 24: 101043.

Chakraborty, B., Modak, P., Banerjee, S. Hydrogen storage in yttrium-decorated single walled carbon nanotube. The Journal of Physical Chemistry C, 2012, 116(42): 22502-22508.

Chandrakumar, K. R. S., Ghosh, S. K. Alkali-metal-induced enhancement of hydrogen adsorption in C_{60} fullerene: An ab initio study. Nano Letters, 2008, 8(1): 13-19.

Chai, J., Head-Gordon, M. Long-range corrected hybrid density functionals with damped atom-atom dispersion corrections. Physical Chemistry Chemical Physics, 2008, 10(44): 6615-6620.

Cruz-Martínez, H., García-Hilerio, B., Montejo-Alvaro, F., et al. Density functional theory-based approaches to improving hydrogen storage in graphene-based materials. Molecules, 2024, 29(2): 436.

Chung, C., Ihm, J., Lee, H. Recent progress on Kubas-type hydrogen-storage nanomaterials: From theories to experiments. Journal of the Korean Physical Society, 2015, 66(11): 1649-1655.

Choudhary, A., Malakkal, L., Siripurapu, R. K., et al. First principles calculations of hydrogen storage on Cu and Pd-decorated graphene. International Journal of Hydrogen Energy, 2016, 41(39): 17652-17656.

de Lara-Castells, M. P., Mitrushchenkov, A. O. Nuclear bound states of molecular hydrogen physisorbed on graphene: An effective two-dimensional model. The Journal of Physical Chemistry A, 2015, 119(44): 11022-11032.

Durgun, E., Ciraci, S., Yildirim, T. Functionalization of carbon-based nanostructures with light transition-metal atoms for hydrogen storage. Physical Review B-Condensed Matter and Materials Physics, 2008, 77(8): 085405.

Durgun, E., Jang, Y., Ciraci, S. Hydrogen storage capacity of Ti-doped boron-nitride and B/Be-substituted carbon nanotubes. Physical Review B-Condensed Matter and Materials Physics, 2007, 76(7): 073413.

Denis, P. A. Investigation of H_2 physisorption on corannulene ($C_{20}H_{10}$), tetraindenocorannulene ($C_{44}H_{18}$), pentaindeno-corannulene ($C_{50}H_{20}$), C_{60}, and their nitrogen derivatives. The Journal of Physical Chemistry C, 2008, 112(7): 2791-2796.

Della, T. D., Suresh, C. H. Sumanene: An efficient π-bowl for dihydrogen storage. Physical Chemistry Chemical Physics, 2018, 20(9): 6227-6235.

Domínguez-Gutiérrez, F. J., Martínez-Flores, C., Krstic, P. S., et al. Theoretical study of the formation of $C_{18}H$ and $C_{18}H_2$ molecules by low energy irradiation with atomic and molecular hydrogen. Radiation Physics and Chemistry, 2021, 179: 109166.

Eslami, M., Moradi, M., Moradi, R. DFT investigation of hydrogen adsorption on the C_3N nanotube. Vacuum, 2016, 133: 7-12.

Eno, E. A., Louis, H., Akpainyang, P. S., et al. Molecular modeling of Cu^-, Ag^-, and Au-decorated aluminum nitride nanotubes for hydrogen storage application. ACS Applied Energy Materials, 2023, 6(8): 4437-4452.

Er, S., de Wijs, G. A., Brocks, G. Improved hydrogen storage in Ca-decorated boron heterofullerenes: A theoretical study. Journal of Materials Chemistry A, 2015, 3(15): 7710-7714.

Faye, O., Hussain, T., Karton, A., et al. Tailoring the capability of carbon nitride (C_3N) nanosheets toward hydrogen storage upon light transition metal decoration. Nanotechnology, 2019, 30(7): 075404.

Germain, J., Fréchet, J. M., Svec, F. Nanoporous polymers for hydrogen storage. Small, 2009, 5(10): 1098-1111.

Guo, T., Jin, C., Smalley, R. E. Doping bucky: F ormation and properties of boron-doped buckminsterfullerene. The Journal of Physical Chemistry, 1991, 22(39).

Gaboardi, M., Pratt, F., Milanese, C., et al. The interaction of hydrogen with corannulene, a promising new platform for energy storage. Carbon, 2019, 155: 432-437.

Han, S., Lee, H. Adsorption properties of hydrogen on (10, 0) single-walled carbon nanotube through density functional theory. Carbon, 2004, 42(11): 2169-2177.

Hultman, L., Stafström, S., Czigány, Z., et al. Cross-linked nano-onions of carbon nitride in the solid phase: Existence of a novel C_{48} N_{12} Aza-fullerene. Physical review letters, 2001, 87(22): 225503.

Hoang, T. K., Antonelli, D. M. Exploiting the Kubas interaction in the design of hydrogen storage materials. Advanced Materials, 2009, 21(18): 1787-1800.

Jhi, S., Kwon, Y. K. Hydrogen adsorption on boron nitride nanotubes: A path to room-temperature hydrogen storage. Physical Review B-Condensed Matter and Materials Physics, 2004, 69(24): 245407.

Janjua, M. R. S. A. Theoretical framework for encapsulation of inorganic $B_{12}N_{12}$ nanoclusters with alkaline earth metals for efficient hydrogen adsorption: A step forward toward hydrogen storage materials. Inorganic Chemistry, 2021, 60(4): 2816-2828.

Kim, G., Jhi, S., Lim, S., et al. Crossover between multipole Coulomb and Kubas interactions in hydrogen adsorption on metal-graphene complexes. Physical Review B-Condensed Matter and Materials Physics, 2009, 79(15): 155437.

Kumar, E. M., Sinthika, S., Thapa, R. First principles guide to tune h-BN nanostructures as superior light-element-based hydrogen storage materials: Role of the bond exchange spillover mechanism. Journal of Materials Chemistry A, 2015, 3(1): 304-313.

Krasnov, P. O., Ding, F., Singh, A. K., et al. Clustering of Sc on SWNT and reduction of hydrogen uptake: Ab-initio all-electron calculations. The Journal of Physical Chemistry C, 2007, 111(49): 17977-17980.

Kim, Y., Zhao, Y., Williamson, A., et al. Nondissociative adsorption of H_2 molecules in light-element-doped fullerenes. Physical Review Letters, 2006, 96(1): 016102.

Komatsu, K., Murata, M., Murata, Y. Encapsulation of molecular hydrogen in fullerene C_{60} by organic synthesis. Science, 2005, 307(5707): 238-240.

Kaiser, K., Scriven, L. M., Schulz, F., et al. An sp-hybridized molecular carbon allotrope, cyclo [18] carbon. Science, 2019, 365(6459): 1299-1301.

Kuang, A., Wang, G., Li, Y., et al. Ab initio investigation of the adsorption of atomic and molecular hydrogen on AlN nanotubes. Applied Surface Science, 2015, 346: 24-32.

Langmi, H. W., Book, D., Walton, A., et al. Hydrogen storage in ion-exchanged zeolites. Journal of Alloys and Compounds, 2005, 404: 637-642.

Luo, Z., Fan, X., Pan, R., et al. A first-principles study of Sc-decorated graphene with pyridinic-N defects for hydrogen storage. International Journal of Hydrogen Energy, 2017, 42(5): 3106-3113.

Lei, W., Zhang, H., Wu, Y., et al. Oxygen-doped boron nitride nanosheets with excellent performance in hydrogen storage. Nano Energy, 2014, 6: 219-224.

Lyu, J., Kudiiarov, V., Lider, A. An overview of the recent progress in modifications of carbon nanotubes for hydrogen adsorption. Nanomaterials, 2020, 10(2): 255.

Liu, W., Zhao, Y., Li, Y., et al. Enhanced hydrogen storage on

Li-dispersed carbon nanotubes. The Journal of Physical Chemistry C, 2009, 113(5): 2028-2033.

Lee, H., Ihm, J., Cohen, M. L., et al. Calcium-decorated carbon nanotubes for high-capacity hydrogen storage: first-principles calculations. Physical Review B-Condensed Matter and Materials Physics, 2009, 80(11): 115412.

Lu, T. , Chen, F. Multiwfn: A multifunctional wavefunction analyzer. Journal of Computational Chemistry, 2012, 33(5): 580-592.

Mattera, L., Rosatelli, F., Salvo, C., et al. Selective adsorption of $1\,H_2$ and $2\,H_2$ on the (0001) graphite surface. Surface Science, 1980, 93(2-3): 515-525.

Ma, L., Wang, L., Sun, Y., et al. First-principles study of hydrogen storage on Ca-decorated defective boron nitride nanosheets. Physica E: Low-dimensional Systems and Nanostructures, 2021, 128: 114588.

Ma, R., Bando, Y., Zhu, H., et al. Hydrogen uptake in boron nitride nanotubes at room temperature. Journal of the American Chemical Society, 2002, 124(26): 7672-7673.

Moradi, M., Naderi, N. First principle study of hydrogen storage on the graphene-like aluminum nitride nanosheet. Structural Chemistry, 2014, 25(4): 1289-1296.

Mpourmpakis, G., Froudakis, G. E. Why boron nitride nanotubes are preferable to carbon nanotubes for hydrogen storage?: An ab initio theoretical study. Catalysis today, 2007, 120(3-4): 341-345.

Mananghaya, M., Yu, D., Santos, G. N. Hydrogen adsorption on boron nitride nanotubes functionalized with transition metals. International Journal of Hydrogen Energy, 2016, 41(31): 13531-13539.

Ma, L., Sun, Y., Wang, L., et al. Calcium decoration of boron nitride nanotubes with vacancy defects as potential hydrogen storage materials: A first-principles investigation. Materials Today Communications, 2021, 26: 101985.

Nachimuthu, S., Lai, P., Jiang, J. Efficient hydrogen storage in boron doped graphene decorated by transition metals-A first-principles study. Carbon, 2014, 73: 132-140.

Noura, M., Rahdar, A., Taimoory, S. M., et al. A theoretical first principles computational investigation into the potential of aluminum-doped boron nitride nanotubes for hydrogen storage. International Journal of Hydrogen Energy, 2020, 45(19): 11176-11189.

Noura, M., Kosar, M., Rahdar, A., et al. Hydrogen adsorption on magnesium-decorated (3, 3) and (5, 0) boron nitride nanotubes. International Journal of Hydrogen Energy, 2023, 48(89): 34862-34873.

Nakamura, T., Ishikawa, K., Yamamoto, K., et al. Synthesis of heterofullerenes by laser ablation. Physical Chemistry Chemical Physics, 1999, 1(10): 2631-2633.

Nair, R. G. S., Nair, A. K. N., Sun, S. Adsorption of drugs on $B_{12}N_{12}$ and $Al_{12}N_{12}$ nanocages. RSC Advances, 2024, 14(43): 31756-31767.

Nair, R. G. S., Nair, A. K. N., Sun, S., et al. Adsorption of organic pollutants on $B_{12}N_{12}$ and $Al_{12}N_{12}$ nanocages. Computational and Theoretical Chemistry, 2025, 1248: 115187.

Nair, R. G. S., Nair, A. K. N., Sun, S. Adsorption of gases on $B_{12}N_{12}$ and $Al_{12}N_{12}$ nanocages. New Journal of Chemistry, 2024, 48(18): 8093-8105.

Otero, G., Biddau, G., Sánchez-Sánchez, C., et al. Fullerenes from aromatic precursors by surface-catalysed cyclodehydrogenation. Nature, 2008, 454(7206): 865-868.

Oku, T., Nishiwaki, A., Narita, I. Formation and atomic structure of $B_{12}N_{12}$ nanocage clusters studied by mass spectrometry and cluster calculation. Science and Technology of Advanced Materials, 2004, 5(5-6): 635-638.

Parambhath, V. B., Nagar, R., Ramaprabhu, S. Effect of nitrogen doping on hydrogen storage capacity of palladium decorated graphene. Langmuir, 2012, 28(20): 7826-7833.

Pradeep, T., Vijayakrishnan, V., Santra, A. K., et al. Interaction of nitrogen with fullerenes: Nitrogen derivatives of C_{60} and C_{70}. The Journal of Physical Chemistry, 1991, 95(26): 10564-10565.

Pupysheva, O. V., Farajian, A. A., Yakobson, B. I. Fullerene nanocage capacity for hydrogen storage. Nano Letters, 2008, 8(3): 767-774.

Petrushenko, I. K., Petrushenko, K. B. Adsorption of diatomic molecules on graphene, h-BN and their BNC heterostructures: DFT study. Diamond and Related Materials, 2019, 100: 107575.

Prinzbach, H., Weiler, A., Landenberger, P., et al. Gas-phase production and photoelectron spectroscopy of the smallest fullerene, C_{20}. Nature, 2000, 407(6800): 60-63.

Rubeš, M., Bludský, O. DFT/CCSD (T) investigation of the interaction of molecular hydrogen with carbon nanostructures. ChemPhysChem, 2009, 10(11): 1868-1873.

Rubeš, M., Kysilka, J., Nachtigall, P., et al. DFT/CC investigation of physical adsorption on a graphite (0001) surface. Physical Chemistry Chemical Physics, 2010, 12(24): 6438-6444.

Suh, M. P., Park, H. J., Prasad, T. K., et al. Hydrogen storage in metal-organic frameworks. Chemical Reviews, 2012, 112(2): 782-835.

Shiraz, H. G., Tavakoli, O. Investigation of graphene-based systems for hydrogen storage. Renewable and Sustainable Energy Reviews, 2017, 74: 104-109.

Singla, M., Jaggi, N. Theoretical investigations of hydrogen gas sensing and storage capacity of graphene-based materials: A review. Sensors and Actuators A: Physical, 2021, 332: 113118.

Spyrou, K., Gournis, D., Rudolf, P. Hydrogen storage in graphene-based materials: Efforts towards enhanced hydrogen absorption. ECS Journal of Solid State Science and Technology, 2013, 2(10): M3160-M3169.

Shevlin, S. A., Guo, Z. X. Density functional theory simulations of complex hydride and carbon-based hydrogen storage materials. Chemical Society Reviews, 2009, 38(1): 211-225.

Sawant, S. V., Patwardhan, A. W., Joshi, J. B., et al. Boron doped carbon nanotubes: Synthesis, characterization and emerging applications–a review. Chemical Engineering Journal, 2022, 427: 131616.

Sun, Q., Wang, Q., Jena, P., et al. Clustering of Ti on a C_{60} surface and its effect on hydrogen storage. Journal of the American Chemical Society, 2005, 127(42): 14582-14583.

Singla, M., Jaggi, N. Enhanced hydrogen sensing properties in copper decorated nitrogen doped defective graphene nanoribbons: DFT study. Physica E: Low-dimensional Systems and Nanostructures, 2021, 131: 114756.

Shevlin, S. A., Guo, Z. X. Hydrogen sorption in defective hexagonal BN sheets and BN nanotubes. Physical Review B-Condensed Matter and Materials Physics, 2007, 76(2): 024104.

Schimmel, H. G., Kearley, G. J., Nijkamp, M. G., et al. Hydrogen adsorption in carbon nanostructures: Comparison of nanotubes, fibers, and coals. Chemistry-A European Journal, 2003, 9(19): 4764-4770.

Seenithurai, S., Pandyan, R. K., Kumar, S. V., et al. Al-decorated carbon nanotube as the molecular hydrogen storage medium. International Journal of Hydrogen Energy, 2014, 39(23): 11990-11998.

Satawara, A. M., Shaikh, G. A., Gupta, S. K., et al. Alkali and transition metals decorated hexagonal boron nitride nanotube in hydrogen storage application. International Journal of Hydrogen Energy, 2024, 87: 1461-1473.

Sahoo, R. K., Chakraborty, B., Sahu, S. Reversible hydrogen storage on alkali metal (Li and Na) decorated C_{20} fullerene: A density functional study. International Journal of Hydrogen Energy, 2021, 46(80): 40251-40261.

Sun, Q., Wang, Q., Jena, P. Functionalized heterofullerenes for hydrogen storage. Applied Physics Letters, 2009, 94(1).

Srinivasu, K., Ghosh, S. K. Transition metal decorated porphyrin-like porous fullerene: Promising materials for molecular hydrogen adsorption. The Journal of Physical Chemistry C, 2012, 116(48): 25184-25189.

Sun, L., Zheng, W., Kang, F., et al. On-surface synthesis and characterization of anti-aromatic cyclo [12] carbon and cyclo [20] carbon. Nature Communications, 2024, 15(1): 7649.

Suresh, C. H., Remya, G. S., Anjalikrishna, P. K. Molecular electrostatic potential analysis: A powerful tool to interpret and predict chemical reactivity. Wiley Interdisciplinary Reviews: Computational Molecular Science, 2022, 12(5): e1601.

Spisak, S. N., Wei, Z., O'Neil, N. J., et al. Convex and concave encapsulation of multiple potassium ions by sumanenyl anions. Journal of the American Chemical Society, 2015, 137(31): 9768-9771.

Trzesowska, N., Wysokiński, R., Michalczyk, M., et al. Trapping of small molecules within single or double cyclo [18] carbon rings. Molecules, 2023, 28(5): 2157.

Frisch, M. J., Trucks, G. W., Schlegel, H. B., et al. Gaussian 16 Rev C 02. Gaussian, Inc Wallingford, CT. 2016.

Tsipas, P., Kassavetis, S., Tsoutsou, D., et al. Evidence for graphite-like hexagonal AlN nanosheets epitaxially grown on single crystal Ag (111). Applied Physics Letters, 2013, 103(25): 251605.

Tang, C., Bando, Y., Ding, X., et al. Catalyzed collapse and enhanced hydrogen storage of BN nanotubes. Journal of the American Chemical Society, 2002, 124(49): 14550-14551.

Tondare, V. N., Balasubramanian, C., Shende, S. V., et al. Field emission from open ended aluminum nitride nanotubes. Applied Physics Letters, 2002, 80(25): 4813-4815.

U. S. Department of Energy. Funding opportunities: DOE Technical targets for onboard hydrogen storage for light-duty vehicles. Alternative Fuels and Feedstocks Office.

Vidali, G., Ihm, G., Kim, H. Y., et al. Potentials of physical adsorption. Surface Science Reports, 1991, 12(4): 135-181.

Venkataramanan, N. S., Khazaei, M., Sahara, R., et al. First-principles study of hydrogen storage over Ni and Rh doped BN sheets. Chemical Physics, 2009, 359(1-3): 173-178.

Valencia, H., Gil, A., Frapper, G. Trends in the hydrogen activation and storage by adsorbed 3d transition metal atoms onto graphene and nanotube surfaces: A DFT study and molecular orbital analysis. The Journal of Physical Chemistry C, 2015, 119(10): 5506-5522.

Wang, S., Liu, C., Zhu, Y. Boosting ambient hydrogen storage in graphene via structural and functional designs: A review. Advanced Energy and Sustainability Research, 2025, 6(6): 2400362.

Wei, D., Liu, Y., Wang, Y., et al. Synthesis of N-doped graphene by chemical vapor deposition and its electrical properties. Nano Letters, 2009, 9(5): 1752-1758.

Wang, X., Sun, G., Routh, P., et al. Heteroatom-doped graphene materials: Syntheses, properties and applications. Chemical Society Reviews, 2014, 43(20): 7067-7098.

Wu, X., Yang, J., Hou, J., et al. Defects-enhanced dissociation of H_2 on boron nitride nanotubes. The Journal of Chemical Physics, 2006, 124(5).

Wang, X., Qi, H., Ma, L., et al. Superalkali NLi_4 anchored on BN sheets for reversible hydrogen storage. Applied Physics Letters, 2021, 118(9).

Wang, L., Zhang, Z., Ma, L., et al. First-principles study of hydrogen storage on Li, Na and K-decorated defective boron nitride nanosheets. The European Physical Journal B, 2022, 95(3): 50.

Wang, T., Wang, C., Huo, Y., et al. Hydrogen storage in C-doped h-BN decorated with titanium atom: A computational study. Chemical Physics Letters, 2022, 803: 139853.

Wu, Q., Hu, Z., Wang, X., et al. Synthesis and characterization of faceted hexagonal aluminum nitride nanotubes. Journal of the American Chemical Society, 2003, 125(34): 10176-10177.

Wang, Q., Sun, Q., Jena, P., et al. Potential of AlN nanostructures as hydrogen storage materials. ACS Nano, 2009, 3(3): 621-626.

Wu, H., Zhang, F., Xu, X., et al. Geometric and energetic aspects of aluminum nitride cages. The Journal of Physical Chemistry A, 2003, 107(1): 204-209.

Wang, G., Yuan, H., Kuang, A., et al. High-capacity hydrogen storage in Li-decorated (AlN)n (n = 12, 24, 36) nanocages. International Journal of Hydrogen Energy, 2014, 39(8): 3780-3789.

Yao, X., Nair, A. K. N., Ruslan, M. F. A. C., et al. Interfacial properties of the hydrogen + brine system in the presence

of hydrophilic silica. International Journal of Hydrogen Energy, 2025, 101: 741-749.

Yeamin, M. B., Faginas-Lago, N., Albertí, M., et al. Multi-scale theoretical investigation of molecular hydrogen adsorption over graphene: Coronene as a case study. RSC Advances, 2014, 4(97): 54447-54453.

Yoon, M., Yang, S., Hicke, C., et al. Calcium as the superior coating metal in functionalization of carbon fullerenes for high-capacity hydrogen storage. Physical Review Letters, 2008, 100(20): 206806.

Yoon, M., Yang, S., Wang, E., et al. Charged fullerenes as high-capacity hydrogen storage media. Nano Letters, 2007, 7(9): 2578-2583.

Ziółkowski, M., Grabowski, S. J., Leszczynski, J. Cooperativity in hydrogen-bonded interactions: Ab initio and "atoms in molecules" analyses. The Journal of Physical Chemistry A, 2006, 110(20): 6514-6521.

Zheng, N., Yang, S., Xu, H., A DFT study of the enhanced hydrogen storage performance of the Li-decorated graphene nanoribbons. Vacuum, 2020, 171: 109011.

Zhang, N., Shi, Y., Li, J., et al. Potential applications of OLi_3-decorated h-BN monosheet for high hydrogen storage. Applied Physics Letters, 2023, 123(8).

Zhou, X., Chu, W., Zhou, Y., et al. DFT simulation on H_2 adsorption over Ni-decorated defective h-BN nanosheets. Applied Surface Science, 2018, 439: 246-253.

Zhang, X., Liu, Z., Hark, S. Synthesis and optical characterization of single-crystalline AlN nanosheets. Solid State Communications, 2007, 143(6-7): 317-320.

Zhao, J., Buldum, A., Han, J., et al. Gas molecule adsorption in carbon nanotubes and nanotube bundles. Nanotechnology, 2002, 13(2): 195-200.

Zhou, Z., Gao, X., Yan, J., et al. Doping effects of B and N on hydrogen adsorption in single-walled carbon nanotubes through density functional calculations. Carbon, 2006, 44(5): 939-947.

Zhou, J., Wang, Q., Sun, Q., et al. Enhanced hydrogen storage on Li functionalized BC_3 nanotube. The Journal of Physical Chemistry C, 2011, 115(13): 6136-6140.

Yildirim, T., Ciraci, S. Titanium-decorated carbon nanotubes as a potential high-capacity hydrogen storage medium. Physical Review Letters, 2005, 94(17): 175501.

Zhang, Z., Zheng, W., Jiang, Q. Hydrogen adsorption on Ce/BNNT systems: A DFT study. International Journal of Hhydrogen Energy, 2012, 37(6): 5090-5099.

Zhang, L., Wu, P., Sullivan, M. B. Hydrogen adsorption on Rh, Ni, and Pd functionalized single-walled boron nitride nanotubes. The Journal of Physical Chemistry C, 2011, 115(10): 4289-4296.

Zimmermann, U., Malinowski, N., Näher, U., et al. Multilayer metal coverage of fullerene molecules. Physical Review Letters, 1994, 72(22): 3542.

Zhao, Y., Kim, Y. H., Dillon, A. C., et al. Hydrogen storage in novel organometallic buckyballs. Physical Review Letters, 2005, 94(15): 155504.

Zhang, Y., Scanlon, L. G., Rottmayer, M. A., et al. Computational investigation of adsorption of molecular hydrogen on lithium-doped corannulene. The Journal of Physical Chemistry B, 2006, 110(45): 22532-22541.

Zhang, Y., Zheng, X., Zhang, S., et al. Bare and Ni decorated $Al_{12}N_{12}$ cage for hydrogen storage: A first-principles study. International Journal of Hydrogen Energy, 2012, 37(17): 12411-12419.

Zhang, J., Qi, P., Zheng, X. Theoretical study of hydrogen storage in Li-decorated $Al_{12}N_{12}$ clusters. Computational and Theoretical Chemistry, 2024, 1236: 114607.